A CFAR Adaptive Matched Filter Detector

FRANK C. ROBEY

DANIEL R. FUHRMANN
Washington University

EDWARD J. KELLY
M.I.T. Lincoln Laboratory

RAMON NITZBERG
General Electric

An adaptive algorithm for radar target detection using an antenna array is proposed. The detector is derived in a manner similar to that of the generalized likelihood-ratio test (GLRT) but contains a simplified test statistic that is a limiting case of the GLRT detector. This simplified detector is analyzed for performance to signals on boresight, as well as when the signal direction is misaligned with the look direction.

Manuscript received August 14, 1989; revised July 20, 1990 and March 23, 1991.

IEEE Log No. 9103598.

This work was funded in part by the Department of Air Force under ESD Contract F19628-85-C-0002.

Authors' addresses: F. C. Robey and D. R. Fuhrmann, Electronic Systems and Signals Research Laboratory, Department of Electrical Engineering, Washington University, St. Louis, MO 63130; E. J. Kelly, M.I.T. Lincoln Laboratory, 244 Wood Street, Lexington, MA 02173; R. Nitzberg, General Electric Co., CSP4-5, Syracuse, NY 13221.

I. INTRODUCTION

In references [4–7], the formulation and analysis of a decision rule for target presence was derived for a radar using an array antenna, under the assumption of Gaussian noise with unknown covariance. It was assumed that a single N-length data vector (called the "primary" vector) may contain a signal or target return with known direction vector $\mathbf{s}$ and unknown complex amplitude b, while $K > N$ other independent data vectors (called "secondary" vectors) are available that are zero mean, and share the same $N \times N$ covariance matrix $\mathbf{M}$. The generalized likelihood ratio test (GLRT) derived under these assumptions is given by

$$\frac{|\mathbf{s}^\dagger \hat{\mathbf{M}}^{-1}\mathbf{z}|^2}{\mathbf{s}^\dagger \hat{\mathbf{M}}^{-1}\mathbf{s}\left(1+\frac{1}{K}\mathbf{z}^\dagger \hat{\mathbf{M}}^{-1}\mathbf{z}\right)} \underset{H_0}{\overset{H_1}{\gtrless}} K\gamma. \tag{1}$$

In this formula $\mathbf{z}$ is the primary data vector, and $\hat{\mathbf{M}}$ is a sample covariance matrix based on the secondary data vectors:

$$\hat{\mathbf{M}} = \frac{1}{K}\sum_{k=1}^{K} \mathbf{z}(k)\mathbf{z}(k)^\dagger. \tag{2}$$

Similar detection problems leading to the same test statistic will also arise for other signal models. For example, the data vector can be modeled as a vector of multiple "looks" at a moving target where the phase shift between elements of the vector corresponds to a Doppler progression. The secondary data may then be taken as samples of data from other ranges.

The test described by (1) is a constant false alarm rate (CFAR) detector, in which the probability of false alarm is independent of the true covariance matrix of the interference. The adaptive detector of Reed, Mallett, and Brennan (RMB) [8] used conventionally for interference rejection is the numerator of this test statistic.

Here, a detection algorithm is derived that is based on the GLRT assuming the covariance is known. After the test statistic is derived, the maximum likelihood estimate of the covariance matrix based on the secondary data is inserted in place of the known covariance. The resulting test statistic has the form of a normalized matched filter and it is also a CFAR detector. This test statistic does not contain the factor in parentheses, found in the denominator of the GLRT (1). This term is computationally intensive for real time systems, as it must be calculated for each new input sample. We note that this term tends to unity when K is large.

The performance of our detector is determined for signals on boresight (i.e., in the $\mathbf{s}$ direction), as well as for signals that are not matched to boresight. The performance of this test to signals that are aligned with the steering vector exhibits a small loss when compared with the GLRT detector at low signal-to-noise ratios (SNR). The new detector exhibits the interesting

property that the probability of detection (PD) is higher than that of the GLRT detector for high SNRs. The GLRT has no known optimality property, and this result demonstrates that the GLRT is not optimal in the Neyman-Pearson sense of maximizing the PD for a given probability of false alarm (PFA). However, the absence of the denominator term causes our test to be much more sensitive to signals that would appear in the sidelobes of the adapted antenna pattern.

II. ADAPTIVE MATCHED FILTER

The same signal model as that used in [5] is assumed. The signal vector $\mathbf{z}$ is assumed to be a complex Gaussian random vector with mean $\mathbf{0}$ under hypothesis H_0, mean $b\mathbf{s}$ under hypothesis H_1, and covariance $\mathbf{M}$. K additional data vectors are available that are assumed to have mean $\mathbf{0}$ and covariance $\mathbf{M}$. These vectors may be used as secondary vectors to estimate the noise covariance.

The procedure used to derive the test statistic is to assume that the covariance is known, and then to write the GLRT maximizing over the unknown parameter b. The resulting test statistic is the output power of the standard colored-noise matched filter. The maximum likelihood estimate of the covariance based on the secondary data alone is then substituted into this test.

The derivation is begun by writing the GLRT

$$\Lambda = \frac{\max_b f_{\mathbf{z}|H_1}(\mathbf{z}; b \mid H_1)}{f_{\mathbf{z}|H_0}(\mathbf{z} \mid H_0)} \underset{H_0}{\overset{H_1}{\gtrless}} \gamma. \tag{3}$$

Substituting the complex multivariate Gaussian density functions and canceling common terms yields

$$\Lambda = e^{-(\mathbf{z}-b\mathbf{s})^\dagger \mathbf{M}^{-1}(\mathbf{z}-b\mathbf{s}) + \mathbf{z}^\dagger \mathbf{M}^{-1}\mathbf{z}}. \tag{4}$$

We can now take the logarithm, and simplify to

$$\log(\Lambda) = 2\mathrm{Re}(b^* \mathbf{s}^\dagger \mathbf{M}^{-1}\mathbf{z}) - |b|^2 \mathbf{s}^\dagger \mathbf{M}^{-1}\mathbf{s}. \tag{5}$$

Maximizing this with respect to the unknown complex amplitude b yields

$$\hat{b} = \frac{\mathbf{s}^\dagger \mathbf{M}^{-1}\mathbf{z}}{\mathbf{s}^\dagger \mathbf{M}^{-1}\mathbf{s}}. \tag{6}$$

Substituting (6) into (5) and simplifying produces the test

$$\frac{|\mathbf{s}^\dagger \mathbf{M}^{-1}\mathbf{z}|^2}{\mathbf{s}^\dagger \mathbf{M}^{-1}\mathbf{s}} \underset{H_0}{\overset{H_1}{\gtrless}} \alpha. \tag{7}$$

This test statistic is proportional to the squared magnitude of the output of the colored noise linear matched filter, since the term in the denominator is a constant when the true covariance is known.

If the noise covariance matrix were known, then we would use the detector described by (7). In general, the covariance matrix is unknown and must be accounted for by using adaptive techniques. The GLRT provides one such adaptive approach. We propose to account for not knowing the true covariance by the *ad hoc* procedure of substituting the maximum likelihood estimate based on the secondary data. Reed, Mallett, and Brennan used a similar approach in their maximum signal-to-noise formulation of the detection problem. The test form is then

$$\frac{|\mathbf{s}^\dagger \hat{\mathbf{M}}^{-1}\mathbf{z}|^2}{\mathbf{s}^\dagger \hat{\mathbf{M}}^{-1}\mathbf{s}} \underset{H_0}{\overset{H_1}{\gtrless}} \alpha. \tag{8}$$

We call this test the adaptive matched filter (AMF) test. This test statistic has the RMB test statistic as the numerator, with a normalization that is the same as that which would be provided by the GLRT for a large number of secondary samples. This normalization will provide the desired CFAR behavior, and is a natural normalization factor to use for this purpose.

The AMF test may also be derived by other methods. In Appendix A it is shown that this test statistic also results from a type of cell averaging CFAR where the cell average is made from the outputs of an RMB adaptive beamformer.

The GLRT uses all the data (primary and secondary) in the likelihood maximization under each hypothesis. The AMF test makes no use of the primary vector to estimate the covariance, therefore poorer detection performance might be expected. In the following sections, the performance loss is shown to be small and that, in certain situations, the AMF test will actually outperform the GLRT.

III. CFAR BEHAVIOR

We now show that the AMF test statistic is independent of the true covariance matrix under H_0 and thus it gives a constant false alarm rate test.

Let $\mathbf{u} = \mathbf{M}^{-1/2}\mathbf{s}$, and $\mathbf{y} = \mathbf{M}^{-1/2}\mathbf{z}$. Then the test can be written

$$\frac{|\mathbf{u}^\dagger \mathbf{M}^{1/2}\hat{\mathbf{M}}^{-1}\mathbf{M}^{1/2}\mathbf{y}|^2}{\mathbf{u}^\dagger \mathbf{M}^{1/2}\hat{\mathbf{M}}^{-1}\mathbf{M}^{1/2}\mathbf{u}} = \frac{|\mathbf{u}^\dagger \tilde{\mathbf{M}}^{-1}\mathbf{y}|^2}{\mathbf{u}^\dagger \tilde{\mathbf{M}}^{-1}\mathbf{u}} \underset{H_0}{\overset{H_1}{\gtrless}} \alpha \tag{9}$$

where $\tilde{\mathbf{M}} \equiv \mathbf{M}^{-1/2}\hat{\mathbf{M}}\mathbf{M}^{-1/2}$. $\tilde{\mathbf{M}}$ is subject to the complex Wishart distribution with parameters K, N, and $\mathbf{I}$, which is denoted $CW(K,N;\mathbf{I})$ [2].

Now a unitary transform is defined that rotates the whitened signal vector into the first elementary vector:

$$d\mathbf{e} = \mathbf{U}^\dagger \mathbf{u}, \qquad \mathbf{e} = [1,0,\ldots,0]^\dagger. \tag{10}$$

The first column of $\mathbf{U}$ is the whitened signal vector $\mathbf{u}$, and the other $N-1$ columns form an arbitrary orthonormal basis for the orthogonal complement of the subspace spanned by $\mathbf{u}$. The test then becomes

$$t = \frac{|d\mathbf{e}^\dagger \tilde{\mathbf{C}}^{-1}\mathbf{x}|^2}{d^2 \mathbf{e}^\dagger \tilde{\mathbf{C}}^{-1}\mathbf{e}} = \frac{|\mathbf{e}^\dagger \tilde{\mathbf{C}}^{-1}\mathbf{x}|^2}{\mathbf{e}^\dagger \tilde{\mathbf{C}}^{-1}\mathbf{e}} \underset{H_0}{\overset{H_1}{\gtrless}} \alpha \tag{11}$$

where $\mathbf{x} \equiv \mathbf{U}^\dagger \mathbf{y}$ and $\tilde{\mathbf{C}} \equiv \mathbf{U}^\dagger \tilde{\mathbf{M}} \mathbf{U}$. Then $\mathbf{x}$ is distributed $N(\mathbf{0},\mathbf{I})$ under H_0, and $\mathbf{C}$ is distributed $CW(K,N;\mathbf{I})$.

The actual covariance does not appear in this equation or in the underlying density functions, and thus this is a CFAR test. This test is independent of both the level and the structure of the true covariance, in contrast to the simple unknown level CFAR characteristic of many common CFAR detectors.

IV. GENERALIZATION OF SIGNAL MODEL

The equations to determine the performance of this detector are derived for a general signal case, where the signal may or may not lie in alignment with the look direction. The case where the signal is in alignment then is a simplification of the general signal model. In our model the signal is assumed to lie along some general direction vector $\mathbf{p}$, hence the signal is now normally distributed $N(\mathbf{0},\mathbf{M})$ on H_0 and $N(b\mathbf{p},\mathbf{M})$ on H_1. The steering vector of the array is assumed to be $\mathbf{q}$.

The direction vectors may be normalized so that

$$\mathbf{p}^\dagger\mathbf{p} = \mathbf{q}^\dagger\mathbf{q} = 1 \tag{12}$$

and the following definitions are made

$$A_\mathbf{q}^2 \equiv (\mathbf{q}^\dagger\mathbf{M}^{-1}\mathbf{q}) \tag{13}$$

$$A_\mathbf{p}^2 \equiv (\mathbf{p}^\dagger\mathbf{M}^{-1}\mathbf{p}). \tag{14}$$

Summarizing [6], these terms may be used to describe the SNR. That is, the maximum SNR is

$$\mathrm{SNR}_{\mathbf{qq}} = |b|^2 A_\mathbf{q} \tag{15}$$

attained when the signal lies along the axis for which the detector is steered. When the signal does not lie in the steering direction, then there is an SNR loss. The SNR that results when the array is steered in the direction corresponding to $\mathbf{q}$ is

$$\mathrm{SNR}_{\mathbf{qp}} = |b|^2 \frac{|\mathbf{q}^\dagger\mathbf{M}^{-1}\mathbf{p}|^2}{(\mathbf{q}^\dagger\mathbf{M}^{-1}\mathbf{q})}. \tag{16}$$

The term $\mathbf{q}^\dagger\mathbf{M}^{-1}\mathbf{p}$ can be interpreted as an inner product of $\mathbf{p}$ and $\mathbf{q}$. Thus the inner product measure of distance $\cos\theta$ may be used to relate the SNR to the maximum SNR [7]. We make the definition that

$$a \equiv \mathrm{SNR}_{\mathbf{qp}} = \mathrm{SNR}_{\mathbf{pp}}\cos^2\theta \tag{17}$$

then

$$\cos\theta e^{j\phi} \equiv \frac{(\mathbf{q}^\dagger\mathbf{M}^{-1}\mathbf{p})}{A_\mathbf{p}A_\mathbf{q}}. \tag{18}$$

We can think of $\mathrm{SNR}_{\mathbf{qp}}$ as the SNR in the subspace spanned by the adapted steering direction, and likewise

$$c \equiv \mathrm{SNR}_{\mathbf{pp}}\sin^2\theta \tag{19}$$

can be viewed as the SNR in the orthogonal subspace.

V. PERFORMANCE EVALUATION

A. Derivation of Test Performance

The analysis of this detector is similar to the analysis given in [5], and uses the same notation. Appropriate whitening and unitary transforms are performed to reformulate the AMF test in the statistically equivalent form

$$\Lambda = \frac{|\mathbf{e}^\dagger\mathbf{S}^{-1}\mathbf{z}|^2}{(\mathbf{e}^\dagger\mathbf{S}^{-1}\mathbf{e})} \underset{H_0}{\overset{H_1}{\gtrless}} \alpha. \tag{20}$$

The variable $\mathbf{z}$ has been redefined in this equation to be the whitened rotated primary data vector $\mathbf{x}$ in (11).

The steps made to form this representation are identical to those used to show that the test statistic is independent of the underlying covariance matrix. Here, because of the generalization of the signal model, the actual mean direction vector may not have been transformed to the first elementary vector. With this in mind, $\mathbf{z}$ is now normally distributed $N(\mathbf{0},\mathbf{I})$ under H_0 and $N(bA_\mathbf{p}\mathbf{f},\mathbf{I})$ under H_1. The transformed covariance estimate $\mathbf{S}$ has the complex Wishart distribution $CW(K,N;\mathbf{I})$, and the signal direction vector is given by

$$\mathbf{f} \equiv \frac{1}{A_\mathbf{p}}\mathbf{U}^\dagger\mathbf{M}^{-1/2}\mathbf{p}. \tag{21}$$

The unitary transform U is required to rotate the whitened direction vector to the first elementary vector $\mathbf{e} \equiv [1,0,\ldots,0]^\dagger$. Following [5], the vector $\mathbf{f}$ is decomposed into components parallel and orthogonal to $\mathbf{e}$, and decomposing $\mathbf{S}$ as well:

$$\mathbf{P} = \mathbf{S}^{-1} = \begin{bmatrix} \mathbf{P}_{AA} & \mathbf{P}_{AB} \\ \mathbf{P}_{BA} & \mathbf{P}_{BB} \end{bmatrix} = \begin{bmatrix} \mathbf{S}_{AA} & \mathbf{S}_{AB} \\ \mathbf{S}_{BA} & \mathbf{S}_{BB} \end{bmatrix}^{-1} \tag{22}$$

$$T \equiv (\mathbf{P}_{AA})^{-1} = \mathbf{S}_{AA} - \mathbf{S}_{AB}\mathbf{S}_{BB}^{-1}\mathbf{S}_{BA} \tag{23}$$

$$\mathbf{y} \equiv \mathbf{z}_A - \mathbf{S}_{AB}\mathbf{S}_{BB}^{-1}\mathbf{z}_B \equiv \frac{\mathbf{v}}{\sqrt{\rho}} \tag{24}$$

$$\rho \equiv (1 + \mathbf{z}_B\mathbf{S}_{BB}^{-1}\mathbf{z}_B)^{-1}. \tag{25}$$

The test statistic can now be simplified to the form

$$\frac{|\mathbf{e}^\dagger\mathbf{S}^{-1}\mathbf{z}|^2}{(\mathbf{e}^\dagger\mathbf{S}^{-1}\mathbf{e})} = \frac{|\mathbf{y}|^2}{T} = (1 + \mathbf{z}_B^\dagger\mathbf{S}_{BB}^{-1}\mathbf{z}_B)\frac{|\mathbf{v}|^2}{T} = \frac{|\mathbf{v}|^2}{\rho T}, \tag{26}$$

and thus the test may be expressed

$$|\mathbf{v}|^2 \underset{H_0}{\overset{H_1}{\gtrless}} \alpha\rho T \tag{27}$$

where $\mathbf{v}$ is now normally distributed $N(0,1)$ or $N(\sqrt{\rho}A_\mathbf{p}b\cos\theta,1)$.

The GLRT is expressed in a similar form without the ρ factor in the threshold. T is an independent random variable which is distributed chi-squared (χ^2)

with L complex degrees-of-freedom. Expression (27) has the form of a scalar CFAR test, in which the threshold is multiplied by the random loss-factor ρ.

The density of the loss factor ρ has been derived in [6], and it is given by the formula

$$f(\rho) = e^{-c\rho} \sum_{m=0}^{L+1} \binom{L+1}{m} \frac{(N+L-1)!}{(N+L-1+m)!} \times c^m f_\beta(\rho; L+1, N+m-1) \quad (28)$$

where c is given in (19) and we have defined $L \equiv K+1-N$. The central Beta density function is

$$f_\beta(x; n, m) = \frac{(n+m-1)!}{(n-1)!(m-1)!} x^{n-1}(1-x)^{m-1}. \quad (29)$$

An alternative form for $f(\rho)$ may be derived by expressing $f(\rho)$ in terms of the confluent hypergeometric function, and using Kummer's first transformation [1] to yield [6]

$$f(\rho) = e^{-c} \sum_{m=0}^{\infty} \frac{c^m}{m!} f_\beta(\rho; L+1, N+m-1) \quad (30)$$

with $L \equiv K+1-N$.

B. Evaluation of the Probability of False Alarm

The PFA for the AMF test is calculated when the signal mean is equal to **0**; consequently the orthogonal SNR term c is 0 and the density functions reduce to the central Beta density function. The PFA will then have the same form as the PFA of the GLRT [4, 5] except for the presence of the factor ρ in the threshold. As shown in [7], the PFA for the GLRT is given by

$$\mathrm{PFA}_{\mathrm{GLRT}} = \frac{1}{(1+\alpha)^L} \quad (31)$$

where $\alpha = \gamma/(1-\gamma)$, and γ is the threshold term of (1). To determine the false alarm probability for the AMF test, the term α can be replaced with $\rho\alpha$, and the expectation with respect to the loss factor ρ can be taken to yield

$$\mathrm{PFA}_{\mathrm{AMF}} = \int_0^1 \mathrm{PFA}_{\mathrm{AMF}} \mid \rho f(\rho)\, d\rho = \int_0^1 \frac{f_\beta(\rho; L+1, N-1)}{(1+\alpha\rho)^L} d\rho. \quad (32)$$

This has been evaluated through numerical integration, and also by means of an expansion into an infinite series, integration term by term, and derivation of truncation bounds, with the same results. Iterative procedures based on bisection and Newton's method have been used to find α when a particular PFA is specified.

C. Evaluation of the Probability of Detection

The conditional PD for the AMF test given ρ, may be expressed in a finite sum expression as [3]

$$\mathrm{PD}_{\mathrm{AMF}} \mid \rho = 1 - \frac{1}{(1+\alpha\rho)^L} \sum_{m=1}^{L} \binom{L}{m} \times (\alpha\rho)^m G_m\left(\frac{a\rho}{1+\alpha\rho}\right) \quad (33)$$

where a is the SNR component defined earlier, and where G_m is the incomplete Gamma function

$$G_m(y) \equiv e^{-y} \sum_{k=0}^{m-1} \frac{y^k}{k!}. \quad (34)$$

Unlike the GLRT, the AMF test includes the loss factor in the threshold as well as in the mean or SNR component. The expectation of the PD with respect to the random variable ρ must be taken to evaluate the unconditional PD. The PD can be written as

$$\mathrm{PD}_{\mathrm{AMF}} = 1 - \int_0^1 \frac{1}{(1+\alpha\rho)^L} \sum_{m=1}^{L} \binom{L}{m} \times (\alpha\rho)^m G_m\left(\frac{a\rho}{1+\alpha\rho}\right) f(\rho)\, d\rho. \quad (35)$$

This equation has been directly computed through numerical integration using the finite sum form of the density function (28). Additionally, this equation has been evaluated through the use of the infinite series form of the density function, integration term by term to express the PD as a series expression containing two finite and three infinite series. Bounds for the three infinite series were obtained using methods similar to that of Shnidman [9]. The results using this method were then used to verify the results of the numerical integration.

In order to evaluate the PD numerically, a single routine has been written to evaluate the PD of a scalar CFAR detector:

$$\mathrm{PD}_{\mathrm{CFAR}}(\alpha, a, L) = 1 - \frac{1}{(1+\alpha)^L} \sum_{m=1}^{L} \binom{L}{m} \alpha^m G_m\left(\frac{a}{1+\alpha}\right). \quad (36)$$

The numerical integration technique of finding the unconditional PD consists of repeatedly calling the routine with a and α replaced by $a\rho$ and $\alpha\rho$, weighting the result by $f_\beta(\rho)$, and summing. When this procedure is performed for the AMF test, the equation implemented is

$$\mathrm{PD}_{\mathrm{AMF}} = \Delta\rho \sum_{i=0}^{I-1} \mathrm{PD}_{\mathrm{CFAR}}(i\Delta\rho\alpha, i\Delta\rho a, L) f_\rho(i\Delta\rho), \quad \Delta\rho = \frac{1}{I} \quad (37)$$

with a defined in (17) as the SNR component parallel to the direction vector. I is chosen to yield a suitably small error by successively doubling the number of terms until the probability of detection varies less than some ϵ.

The corresponding equation for the GLRT is numerically integrated in the same manner with the equation implemented being

$$\mathrm{PD}_{\mathrm{GLRT}} = \Delta\rho \sum_{i=0}^{I-1} \mathrm{PD}_{\mathrm{CFAR}}(\alpha, i\Delta\rho a, L) f_\rho(i\Delta\rho). \quad (38)$$

If a in (37) or (38) is now replaced by γa where γ is a random loss, the PD for the Swerling target fluctuation models [10] may be found. For these cases, γ is subject to a χ^2 distribution with the number of degrees of freedom dependent upon the Swerling model chosen. For the Swerling I model, there will be only one complex degree of freedom, and the density function for γ is

$$f_\gamma = e^{-\gamma}. \quad (39)$$

If the expectation with respect to γ is taken on $G_m(\gamma y)$, (34), then

$$\int_0^\infty G_m(\gamma y) f_\gamma \, d\gamma = 1 - \left(\frac{y}{1+y}\right)^m \quad (40)$$

and the conditional PD is then found (after some algebra) to be

$$\mathrm{PD}_{\mathrm{AMF}} \mid \rho = \left(\frac{1+a\rho}{1+(\alpha+a)\rho}\right)^L. \quad (41)$$

This expression can be numerically integrated with respect to the loss factor ρ. Using the same procedure for the GLRT yields

$$\mathrm{PD}_{\mathrm{GLRT}} \mid \rho = \left(\frac{1+a\rho}{1+\alpha+a\rho}\right)^L. \quad (42)$$

In these cases, no signal mismatch is assumed. For comparison, the PD for the Swerling I matched filter is [3]

$$\mathrm{PD}_{\mathrm{MF}} = e^{-\alpha/(1+a)}. \quad (43)$$

VI. PERFORMANCE RESULTS

A. Performance to Matched Signals

In order to gain a better understanding of the detection properties of this detector, we first look at signals aligned with the steering vector. In this case, the loss factor density reduces to the central Beta density, and the loss is dependent only on the dimensional parameters. The density of the loss factor is then

$$f(\rho) = f_\beta(\rho; L+1, N-1). \quad (44)$$

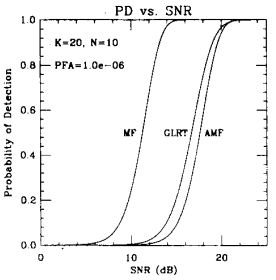

Fig. 1. Probability of detection, $N = 10$, $K = 20$.

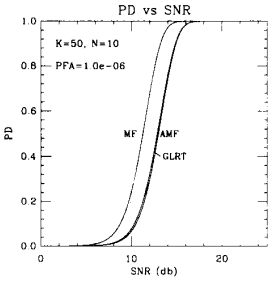

Fig. 2. Probability of detection, $N = 10$, $K = 50$.

Receiver operating characteristic curves are generated by first determining the threshold required to achieve a desired false alarm probability. Using this threshold, the SNR is varied and the PD calculated. Plotting the PD as a function of SNR results in the characterization of a particular test. Some characteristic curves for the known covariance matched-filter detector, the AMF detector and the GLRT detector are plotted in Figs. 1–4. Test parameters are given directly on the figures. The curves for the known covariance were generated using Shnidman's techniques [9] for evaluation of Marcum's Q-function.

From these curves, we can see that there is less than 1 dB additional loss in the AMF detector compared with the GLRT detector. This slight advantage to the GLRT detector decreases at increasing SNRs and there is a crossover in detector performance for signals aligned with the steering vector where the AMF detector has a higher performance. This is shown in the expanded graph of Fig. 5. No claim to optimality is made for the GLRT, and this is one example of a technique that is superior.

Several of the graphs are for $K = 2N$ which corresponds to approximately 3 dB loss in SNR for an adaptive beamformer [8]. We can see from the plots that additional SNR in excess of the 3 dB is required for the adaptive detection algorithms to have a PD that is equal to that of the known covariance detector.

Figs. 6 and 7 illustrate the PD when the Swerling fluctuation is included. The change in the shape of the detection curves is typical of the Swerling model.

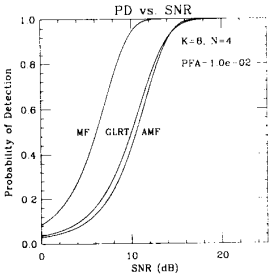

Fig. 3. Probability of detection, $N = 4$, $K = 8$.

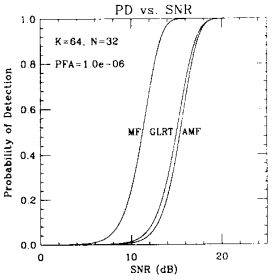

Fig. 4. Probability of detection, $N = 32$, $K = 64$.

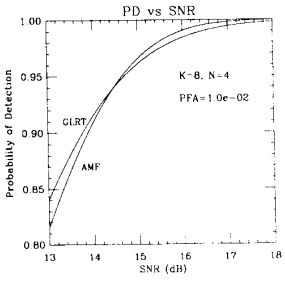

Fig. 5. Probability of detection, $N = 4$, $K = 8$; expanded to show detail.

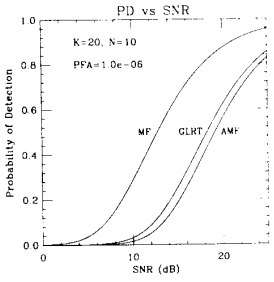

Fig. 6. Swerling I probability of detection, $N = 10$, $K = 20$.

B. Performance to Mismatched Signals

When analyzing the PD curves, one must keep in mind when detection is desired. We desire to detect a target when it is aligned with the steering vector, i.e., when $\cos^2\theta = 1$. When there is significant separation between the steering vector and the target directions, $\cos^2\theta$ will be less than 1 and detection is normally undesirable.

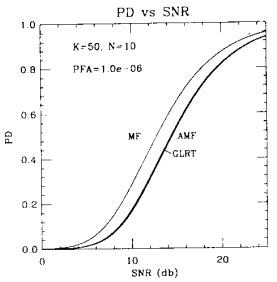

Fig. 7. Swerling I probability of detection, $N = 10$, $K = 50$.

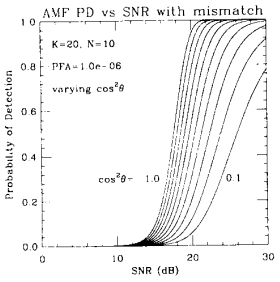

Fig. 8. AMF probability of detection with mismatch, $N = 10$, $K = 20$.

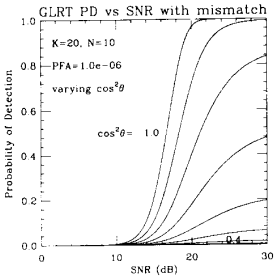

Fig. 9. GLRT probability of detection with mismatch, $N = 10$, $K = 20$.

With this in mind, we discuss Figs. 8–11, the detection curves under mismatched conditions. Here, the PFA is fixed, the mismatch parameter $\cos^2\theta$ is stepped from 0.1 to 1.0 in 0.1 steps, and the PD is calculated as the total SNR is varied. In these plots, the crossover in detector performance (i.e., equal PD for GLRT and AMF with a given value of $\cos^2\theta$) is seen to occur at lower SNRs. This implies a lowering of the PD sidelobes of the GLRT detector at high SNR levels compared with the AMF detector, preventing signals from burning through, and being detected. For large N the first sidelobe for a uniform linear array with receiver only noise is at -13.4 dB or $\cos^2\theta = 0.04503$. There is then a significant difference in sidelobe performance for these two detectors.

In order to point out the performance difference between the detectors, plots of the difference in SNR

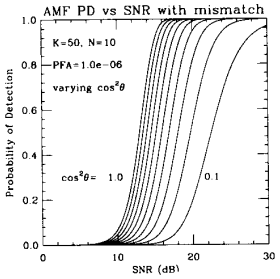

Fig. 10. AMF probability of detection with mismatch, $N = 10$, $K = 50$.

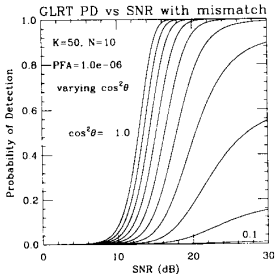

Fig. 11. GLRT probability of detection with mismatch, $N = 10$, $K = 50$.

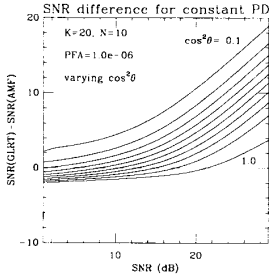

Fig. 12. SNR difference to achieve constant probability of detection, $N = 10$, $K = 20$.

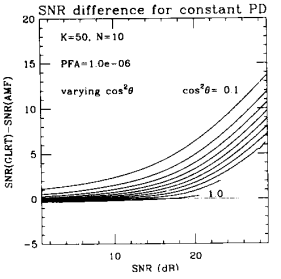

Fig. 13. SNR difference to achieve constant probability of detection, $N = 10$, $K = 50$.

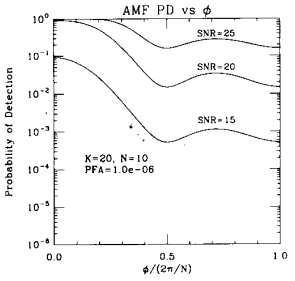

Fig. 14. AMF probability of detection versus angle, $N = 10$, $K = 20$.

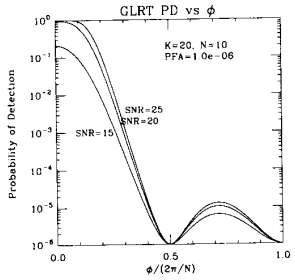

Fig. 15. GLRT probability of detection versus angle, $N = 10$, $K = 20$.

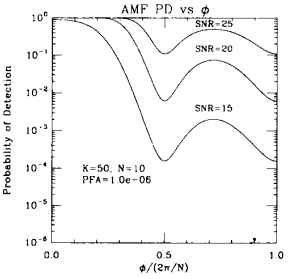

Fig. 16. AMF probability of detection versus angle, $N = 10$, $K = 50$.

required to achieve the PD of the GLRT detector are shown in Figs. 12 and 13. For given PFA and $\cos^2\theta$ values, we vary the SNR, determine the PD for the AMF test then find the additional SNR that is required for the GLRT detector to have the same PD. The crossover points are obvious when the curves are presented in this manner. These points show the superiority of the GLRT detector in rejecting mismatched signals. These plots also show that at low SNR levels, there is no practical difference in the detectors, although the PD is low in this region.

Figs. 14–17 illustrate the mainlobe and first sidelobe for the PD when the covariance is due only to receiver noise. In this case, the loss factor will have the characteristic $\sin(N\phi/2)/\sin(\phi/2)$ response; the argument ϕ of this function is the horizontal axis. The reduction in threshold level for the AMF detector due to mismatch is shown in the increase in the PD in what would be nulls of the $\sin(N\phi/2)/\sin(\phi/2)$ response. The "omnidirectional" characteristic of this detector is also shown by the higher PD as a function of angle.

The difference in the PD at high signal-to-noise levels can be explained by analyzing the test statistics.

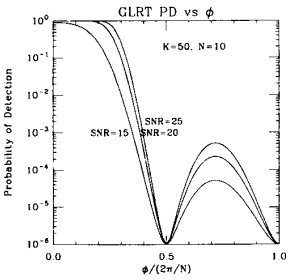

Fig. 17. GLRT probability of detection versus angle, $N = 10$, $K = 50$.

Assume that the true noise covariance is the identity I, and that the estimate of the covariance matrix is perfect. The AMF test statistic then takes the form

$$\frac{|\mathbf{s}^\dagger \mathbf{I}^{-1}\mathbf{z}|^2}{\mathbf{s}^\dagger \mathbf{I}^{-1}\mathbf{s}} = \frac{|\mathbf{s}^\dagger \mathbf{z}|^2}{\mathbf{s}^\dagger \mathbf{s}} = |\mathbf{z}|^2 \cos^2\theta \underset{H_0}{\overset{H_1}{\gtrless}} \gamma. \tag{45}$$

If the signal is not orthogonal to the assumed direction we can rewrite this as

$$|\mathbf{z}|^2 \underset{H_0}{\overset{H_1}{\gtrless}} \frac{\gamma}{\cos^2\theta}. \tag{46}$$

This is compared with the GLRT written in the same form:

$$\frac{|\mathbf{z}|^2}{\left[1 + \frac{1}{K}|\mathbf{z}|^2\right]} \underset{H_0}{\overset{H_1}{\gtrless}} \frac{\gamma}{\cos^2\theta}. \tag{47}$$

The left-hand side of this equation for the GLRT test will approach an asymptote at high SNRs, while for the AMF test, the left hand side is unbounded. The GLRT then will have a maximum separation that will allow detection at a given threshold, while the AMF test will allow large signals that are nearly orthogonal to the steering direction to be detected.

VII. CONCLUSION

We have proposed the AMF detector, a simple alternative to the GLRT detector. Both of these tests are CFAR tests, and have comparable performance to signals aligned with the assumed direction of arrival. The generalized likelihood-ratio test is not optimal in the Neyman–Pearson sense as the AMF test has a probability of detection that is higher than that of the GLRT for some situations. The AMF does not provide the rejection for signals that are misaligned with the assumed direction of arrival as well as the GLRT and this may be undesirable for some applications.

APPENDIX A. ALTERNATE DERIVATION OF AMF TEST STATISTIC

The AMF test statistic can be derived in an alternate manner. Assume that adapted beamforming is performed using the technique of Reed, Mallet, and Brennan [8]. The secondary data for covariance estimation have been taken from the data in other range bins. Now use the beamforming outputs along the boresight from the secondary data in an unknown level CFAR detector:

$$|\mathbf{s}^\dagger \hat{\mathbf{M}}^{-1}\mathbf{z}|^2 \underset{H_0}{\overset{H_1}{\gtrless}} \frac{\alpha}{K} \sum_{i=1}^{K} |\mathbf{s}^\dagger \hat{\mathbf{M}}^{-1}\mathbf{z}(i)|^2. \tag{48}$$

Expanding the right-hand side of (A11) yields

$$|\mathbf{s}^\dagger \hat{\mathbf{M}}^{-1}\mathbf{z}|^2 \underset{H_0}{\overset{H_1}{\gtrless}} \frac{\alpha}{K} \sum_{i=1}^{K} \mathbf{s}^\dagger \hat{\mathbf{M}}^{-1}\mathbf{z}(i)\mathbf{z}(i)^\dagger \hat{\mathbf{M}}^{-1}\mathbf{s}. \tag{49}$$

Now the covariance estimate $\hat{\mathbf{M}}$ may be substituted for the sum of the outer products of the data:

$$|\mathbf{s}^\dagger \hat{\mathbf{M}}^{-1}\mathbf{z}|^2 \underset{H_0}{\overset{H_1}{\gtrless}} \frac{\alpha}{K} K \mathbf{s}^\dagger \hat{\mathbf{M}}^{-1}\hat{\mathbf{M}}\hat{\mathbf{M}}^{-1}\mathbf{s}. \tag{50}$$

The right side can then be simplified to

$$|\mathbf{s}^\dagger \hat{\mathbf{M}}^{-1}\mathbf{z}|^2 \underset{H_0}{\overset{H_1}{\gtrless}} \alpha \mathbf{s}^\dagger \hat{\mathbf{M}}^{-1}\mathbf{s} \tag{51}$$

and this can be written as the AMF test

$$\frac{|\mathbf{s}^\dagger \hat{\mathbf{M}}^{-1}\mathbf{z}|^2}{\mathbf{s}^\dagger \hat{\mathbf{M}}^{-1}\mathbf{s}} \underset{H_0}{\overset{H_1}{\gtrless}} \alpha. \tag{52}$$

ACKNOWLEDGMENT

The authors would like to thank Ken Senne for his guidance and support of this project.

REFERENCES

[1] Abramowitz, M., and Stegun, I. A. (1970)
Handbook of Mathematical Functions.
National Bureau of Standards, Washington, DC, 1970.

[2] Goodman, N. R. (1963)
Statistical analysis based on a certain multivariate complex Gaussian distribution.
Annals of Mathematical Statistics, **34** (Mar. 1963), 152–177.

[3] Kelly, E. J. (1981)
Finite sum expressions for signal detection probabilities.
Technical report 566, M.I.T. Lincoln Laboratories, Lexington, MA, May 1981.

[4] Kelly, E. J. (1985)
Adaptive detection in non-stationary interference, Part I and Part II.
Technical Report 724, M.I.T. Lincoln Laboratories, Lexington, MA, June 1985.

[5] Kelly, E. J. (1986)
An adaptive detection algorithm.
IEEE Transactions on Aerospace and Electronic Systems, **AES-22**, 1 (Mar. 1986), 115.

[6] Kelly, E. J. (1987)
Adaptive detection in non-stationary interference, Part III.
Technical Report 761, M.I.T. Lincoln Laboratories, Lexington, MA, Aug. 1987.

[7] Kelly, E. J. (1989)
Performance of an adaptive detection algorithm: Rejection of unwanted signals.
IEEE Transactions on Aerospace and Electronic Systems, **25**, 2 (Mar. 1989), 122–133.

[8] Reed, I. S., Mallett, S. D., and Brennan, L. E. (1974)
Rapid convergence rate in adaptive arrays.
IEEE Transactions on Aerospace and Electronic Systems, **AES-10**, 6 (Nov. 1974), 853–863.

[9] Shnidman, D. A. (1976)
Efficient evaluation of the probability of detection and the generalized Q-function.
IEEE Transactions on Information Theory, **IT-22** (Nov. 1976), 746.

[10] Skolnik, M. L. (1980)
Introduction to Radar Systems.
New York: McGraw-Hill, 1980.

Frank C. Robey was born in St. Louis, MO on January 30, 1958. He received the BSEE (Summa Cum Laude) in 1979 and the MSEE degree in 1980 from University of Missouri, Columbia. He received the D.Sc. degree in 1990 from Washington University, St. Louis, MO.

He was a member of the technical staff at Hewlett Packard from 1980 to 1984 in Loveland, CO, and Lake Stevens, WA. From 1984 to 1988 he was with Emerson Electric Co. in St. Louis. He is currently a staff member at M.I.T. Lincoln Laboratory, Lexington, MA. His research interests include adaptive and sensor-array signal processing.

Daniel R. Fuhrmann received the BSEE degree in 1979 from Washington University, St. Louis, MO, the MA and MSE degrees in 1982, and the Ph.D. degree in 1984, all from Princeton University, Princeton, NJ.

From 1979 to 1980 he was employed by Telex Computer Products, Tulsa, OK. Since 1984 he has been with the Department of Electrical Engineering, Washington University, St. Louis, MO, where he is currently an Associate Professor. He has also been a Research Associate with the Institute for Biomedical Computing at Washington University. In 1987 he was an ASEE/Navy Summer Faculty Research Fellow with the Naval Underwater Systems Center, New London, CT, and currently he is a consultant with M.I.T. Lincoln Laboratory, Lexington, MA. His research interests include signal processing for sensor arrays, numerical linear algebra, and image compression.

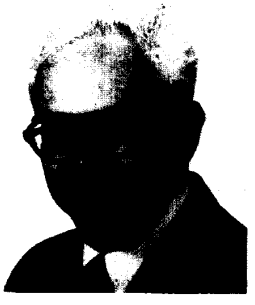

Ramon Nitzberg was born in Brooklyn, NY on November 2, 1929. He received the B.E.E. degree from the City College of New York, in 1950, and the M.E.E. and Ph.D. degrees in electrical engineering from Syracuse University, Syracuse, NY, in 1953 and 1970, respectively.

He was employed at various locations of General Electric since 1951 until his retirement in 1990. Since his retirement, he has engaged in lecturing, independent research, and part-time consulting. His primary interests include signal processing, constant false alarm rate techniques, and adaptive processing.

Dr. Nitzberg is a member of the adjunct faculty of the Electrical and Computer Engineering Department at Syracuse University, a member of Sigma Xi, and a registered Professional Engineer in the State of New York. He is listed in "Who's Who in America".

Edward J. Kelly was born in Philadelphia, PA, in 1924. He received the S.B. degree in 1945, and the Ph.D. degree in 1950, both from the Massachusetts Institute of Technology, Cambridge, MA, in theoretical physics.

He was a staff member at Brookhaven National Laboratory, Upton, NY, from 1950 to 1952, and joined M.I.T. Lincoln Laboratory in 1952, where he is now a member of the Senior Staff.

His work at Lincoln Laboratory has been in the areas of radar detection and estimation theory, applied seismology, air traffic control, spread spectrum communications and, currently, space-based radar systems analysis.